

# A metastable allotropic transformation in Nb induced by planetary ball milling

P.P. Chattopadhyay, S.K. Pabi, I. Manna\*

*Department of Metallurgical and Materials Engineering, Indian Institute of Technology, Kharagpur 721302, West Bengal, India*

## Abstract

The present investigation concerns planetary ball milling of elemental Nb in hardened steel and WC-coated media. Continued milling for about 20 h reduces the grain size below 10 nm with a concomitant lattice expansion. The final product obtained after 30–40 h milling is a pure f.c.c. phase. A detailed micro structural/compositional characterization by X-ray diffraction, resistivity measurements and wet chemical analysis proves that the said f.c.c. phase is neither NbN nor NbC. Instead, it is suggested that elemental Nb undergoes an irreversible b.c.c.  $\rightarrow$  f.c.c. allotropic transformation when the grain size reduces to below 10 nm during high energy ball milling. Furthermore, this f.c.c. phase possibly undergoes an impurity stabilized ordering transformation on annealing at 900°C for 2 h. Finally, the role of impurity in causing this allotropic change is examined. Published by Elsevier Science B.V.

*Keywords:* Ball milling; Allotropic transformation; Ordering; X-ray diffraction; Niobium

## 1. Introduction

Binary/ternary aluminides are considered potential candidates for structural applications at high temperatures due to their high solidus temperature, high specific mechanical strength and excellent oxidation resistance at elevated temperatures [1]. In the past, nickel- [2–4] and iron-based aluminides [5,6] have been successfully synthesized by mechanical alloying. However, similar attempts to synthesize nanocrystalline Nb<sub>3</sub>Al by mechanical alloying have mostly remained unsuccessful [7–9]. For instance, Hellstern et al. [7] have obtained only a nanocrystalline solid solution despite 60 h of milling of a Nb<sub>75</sub>Al<sub>25</sub> powder blend in a planetary ball mill. Recently, Peng et al. [8] have obtained a nanocrystalline f.c.c. phase after 40 h of milling of a Nb<sub>75</sub>Al<sub>25</sub> blend in a Spex-8000 mill. Subsequently, it has been suggested that this f.c.c. phase could be NbN with a lattice parameter of 0.439 nm formed due to nitrogen contamination during milling. It is further proposed that NbN forms through a phase evolution sequence that involves formation of an amorphous alloy marked by a diffused peak after 10 h of milling. However, Rock and Okazaki [9] have earlier demonstrated by a de-convolution analysis that the peak broadening believed to be due to the

amorphous phase could actually be attributed to the coexistence of the overlapping peaks of Nb<sub>3</sub>Al, Nb<sub>2</sub>Al, Nb and Al obtained in the diffractograph following extended hours (~1800 ks) of low energy ball milling of an initial Nb<sub>77</sub>Al<sub>23</sub> composition. In any case, it appears that synthesis of single phase nanocrystalline Nb<sub>3</sub>Al by mechanical alloying remains elusive. Indeed, our own efforts in this direction have substantiated the above inference that mechanical alloying of Nb<sub>75</sub>Al<sub>25</sub> powder blend does not produce pure nanocrystalline Nb<sub>3</sub>Al irrespective of the milling media and speed [10]. In an attempt to understand the reason for this inability and investigate the genesis of the f.c.c. phase produced during milling, a detailed study of high energy ball milling of elemental Nb powder has been undertaken. It will be demonstrated that Nb undergoes a hitherto unknown b.c.c.  $\rightarrow$  f.c.c. allotropic transformation during ball milling in the nanocrystalline state that is identical to the allotropic transformation in the nanocrystalline Ti–Al system [11] and elemental Co [12] detected during a similar ball milling experiment. The possible role of impurity in causing this change will be examined.

## 2. Experimental

Elemental Nb powder having an average particle size of 50  $\mu$ m was suspended in toluene and milled in a Fritsch P5 planetary ball mill at 300 rpm using either hardened steel

\* Corresponding author. Tel.: +91-3222-55221/83266; fax: +91-3222-55303/77190.

E-mail address: imanna@metal.iitkgp.ernet.in (I. Manna).

or WC vials and balls with a ball to powder weight ratio of 10:1. The samples collected at different stages of milling were subjected to a careful X-ray diffraction (XRD) analysis using Co- $K_{\alpha}$  radiation. The average grain size ( $d_c$ ) was determined from peak broadening using the Scherrer equation [13] after elimination of the strain effect by Lorentzian curve-fitting [14] and instrumental effect by comparing the relevant peaks with those from the standard annealed sample (annealed at 773 K for 2 h). In addition, a careful de-convolution analysis was carried out by plotting the second derivative of the XRD intensity distribution as a function of the respective Bragg angles ( $2\theta$ ) to reveal and separate out the constituent/overlapping peaks. The room temperature resistivity of a selected set of milled products was measured by the conventional four probe technique using a DC double Kelvin bridge incorporating the Van der Pauw corrections [15]. Finally, a number of samples were subjected to wet chemical analysis to determine the level of nitrogen and carbon contamination in the milled product introduced during ball milling by the micro-Kjeldahl method [16] and by the combustion method using Strohlein apparatus, respectively.

### 3. Results and discussion

Fig. 1 presents a series of XRD patterns obtained from elemental Nb samples collected at different stages of milling with hardened steel vials and balls. The milled product after 2 h of milling shows only the b.c.c. peaks of Nb. However, the presence of  $(110)_{\text{Fe}}$  peak after 6 h of milling suggests that a measurable amount of Fe contamination has been introduced from the milling media during the ball milling. During subsequent milling, it is apparent that the b.c.c.-Nb peaks undergo both broadening and shifting towards lower  $2\theta$  values with the increase in milling time ( $t$ ). While peak broadening (after eliminating the effects of strain and instrumental errors) may be related to grain size reduction, shifting of the peak positions appears to indicate that lattice expansion accompanies the formation of nanocrystalline state in the present system. In this regard, it may be noted that dissolution of Fe from the milling media cannot ac-

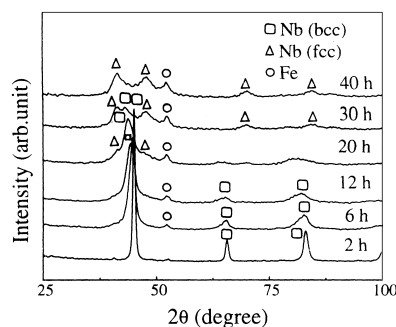


Fig. 1. XRD patterns obtained from Nb powder subjected to milling in steel media for different periods.

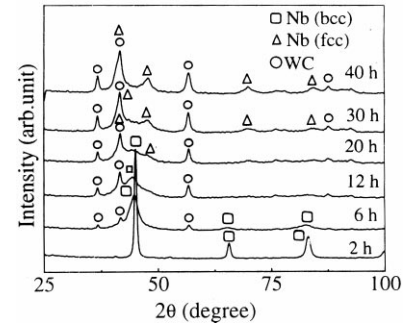


Fig. 2. XRD patterns obtained from Nb powder subjected to milling in WC media for different periods.

count for the lattice expansion of Nb as the atomic diameter of Fe (0.24824 nm) is smaller than that of Nb (0.28637 nm) and both possess b.c.c. Bravais lattice [13].

Fig. 2 presents a similar stack of XRD profiles obtained from ball milling of elemental Nb samples using WC vials and balls for different periods of  $t$ . It is evident that ball milling in WC media yields exactly identical phases as those obtained by milling in steel media under comparable conditions except that the contaminant here is WC instead of Fe as in Fig. 1. In view of this similarity, further analysis in this study has been carried out with samples milled only in the steel media.

It is interesting to note that the XRD patterns of samples milled in either medium at  $t = 40$  h can be indexed only in terms of an f.c.c. phase with an apparent lattice parameter ( $a$ ) of 0.418 nm (obtained from the most intense  $(111)$  peak). Fig. 3 allows determination of the precise lattice parameter ( $a_0$ ) of this f.c.c. phase as 0.428 nm obtained from the variation of  $a$  (determined from the data of Fig. 1) with the Nelson–Riley (N–R) parameter ( $= (\cos^2 \theta / \sin \theta) + \cos^2 \theta / \theta$ ) extrapolated to N–R parameter equal to zero [13]. Thus, it appears that Nb undergoes a b.c.c.  $\rightarrow$  f.c.c. allotropic transformation that reaches its completion at  $t = 40$  h during milling say, in steel vials. Earlier, the appearance of f.c.c.-Nb phase at the expense of b.c.c.-Nb is first noted

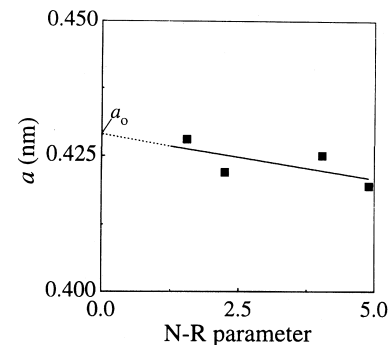


Fig. 3. Extrapolation of the calculated values of  $a$  of f.c.c.-Nb produced by ball milling of b.c.c.-Nb for 40 h in steel vial to obtain the precise lattice parameter ( $a_0$ ).

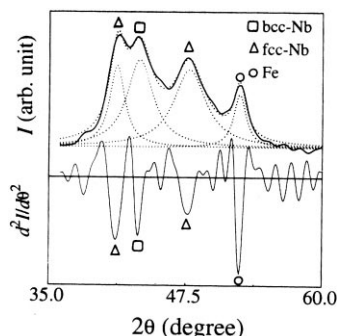


Fig. 4. De-convolution of the overlapping  $(111)_{\text{Nb}}$ ,  $(110)_{\text{Nb}}$  and  $(200)_{\text{Nb}}$  peaks in the XRD profile of elemental Nb obtained by ball milling in steel vial for 30 h.

after  $t = 20$  h of milling. Furthermore, it is interesting to note that the  $(110)_{\text{Nb}}$  peak is unusually broad following milling for  $t = 30$  h and resembles that from an amorphous phase (Fig. 1). In the past, Rock and Okazaki [9] have also noted a similar broad peak in  $\text{Nb}_{77}\text{Al}_{23}$  powder blend following 1800 ks of low energy ball milling. Subsequently, they have attributed this peak broadening to the coexistence of several overlapping peaks due to  $\text{Nb}_3\text{Al}$ ,  $\text{Nb}_2\text{Al}$ , Nb and Al by a de-convolution analysis. In the present study, a similar exercise of de-convolution of the concerned broad peak by plotting  $d^2I/d^2(2\theta)$  against  $2\theta$  (where  $I$  represents the X-ray scattering intensity) reveals that this peak is composed of the  $(111)_{\text{Nb}}$ ,  $(110)_{\text{Nb}}$  and  $(200)_{\text{Nb}}$  peaks (Fig. 4). While the integrated intensity of the f.c.c.- $(111)_{\text{Nb}}$  peak increases as  $t$  increases from 20 to 40 h, the b.c.c.- $(110)_{\text{Nb}}$  peak disappears from the XRD profile at  $t = 40$  h (Fig. 1). Thus, it seems that the b.c.c.  $\rightarrow$  f.c.c. allotropic transformation initiates and reaches completion between 20 and 40 h of milling in steel media in the present study.

Peng et al. [8] have earlier presumed that the similar f.c.c. peaks obtained from  $\text{Nb}_{75}\text{Al}_{25}$  powder blend following 40 h of ball milling were due to the formation of NbN. If the f.c.c. peaks in the present study at  $t = 40$  h are due to NbN, then the latter must have formed during milling as these f.c.c. peaks are absent in the initial stages of milling (Figs. 1 and 2). In order to test this hypothesis, a careful quantitative chemical analysis of the milled product taken from both the milling media after  $t = 40$  h was conducted by micro-Kjeldahl method [16] to estimate the nitrogen content. The results of this chemical analysis revealed that the milled powder contained only 0.11 wt.% nitrogen, which was possibly dissolved from the atmosphere within the vial during milling. Since stoichiometric NbN requires 13.1 wt.% or at least 5 wt.% nitrogen to form the NbN intermetallic phase [17], NbN cannot be the principal constituent of the milled product at  $t = 40$  h in the present study. Furthermore, nitrogen is sparingly soluble in Nb at room temperature and hence cannot account for the XRD peak shifts observed in the present study.

It may be mentioned that the present f.c.c. peaks noted in the XRD patterns (Figs. 1 and 2) are similar to those of NbC reported in the literature. Thus, it may be anticipated that dissociation of toluene (used as a process control reagent in milling) could liberate carbon which might subsequently form NbC by reacting with Nb. However, the wet chemical analysis of the 40 h milled sample shows a maximum of about 2 wt.% carbon (including the carbon from the adsorbed toluene in the powder) which is far lower than the amount of carbon expected (i.e., 10 wt.% [18]) if the final milled product were NbC. Thus, the f.c.c. peaks observed in Figs. 1 and 2 are not due to NbC.

To substantiate the above inferences that the f.c.c. peaks in Figs. 1 and 2 are neither due to NbN nor NbC, the resistivity measurements of the milled products after 20 and 40 h of milling (when the powders contain predominantly b.c.c. and f.c.c. phase, respectively) showed that the room temperature resistivity values of the b.c.c. and f.c.c. phase were 18 and  $3.5 \mu\Omega \text{ mm}$ , respectively. If the f.c.c. phase were an intermetallic compound like NbC or NbN (or a refractory compound as  $\text{NbO}_2$ ), the resistivity of the 40 h milled product would have been far greater than that of the 20 h milled product of a b.c.c. solid solution. It may be noted that the resistivity values obtained from the green compacted samples (with about 80% of the theoretical density) is remarkably higher than the sample for coarse Nb ( $=1.6 \mu\Omega \text{ mm}$ ). Such an increase in resistivity may be attributed to the nanometer size scale of the coherent domain and/or porosity present in the sample.

Fig. 5 shows the reduction in  $d_c$  (calculated from the XRD data of Fig. 1) as a function of  $t$ . It appears that planetary ball milling in steel media reduces the grain size of Nb to nanometric level ( $<20$  nm) in less than 10 h of milling. Furthermore, the rate of decrease in  $d_c$  as a function of  $t$  is faster during the initial stage of milling and is nearly zero as  $d_c$  approaches a minimum value of 8 nm at  $t = 30$  h. However, the appearance of f.c.c.-Nb, which has a marginally higher grain size, coincides with the stage when  $d_c$  for b.c.c.-Nb has decreased below 10 nm (i.e.,  $t > 20$  h).

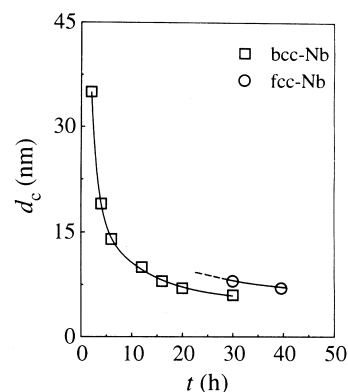


Fig. 5. Variation of grain size ( $d_c$ ) with milling time ( $t$ ) during ball milling of elemental Nb. Note that f.c.c.-Nb appears after 30 h.

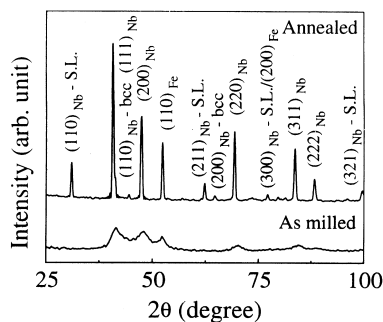


Fig. 6. XRD patterns showing the phase evolution in Nb after milling for 40 h and subsequent annealing at 900°C for 2 h.

Thus, it appears that the b.c.c.  $\rightarrow$  f.c.c. allotropic transition due to milling in steel media is feasible only at  $d_c < 10$  nm.

The XRD patterns in Fig. 6 show that the f.c.c.-Nb phase obtained after 40 h of ball milling in steel media undergoes ordering (as revealed by the superlattice peaks), in addition to grain coarsening (as shown by sharpening of the peaks), following an isothermal annealing at 900°C for 2 h. Furthermore, Fig. 1 reveals the presence of  $\alpha$ -Fe after  $t = 8$  h possibly introduced as a contaminant from the milling media. The ordering transformation noted in Fig. 6 may arise due to the presence of such Fe contamination in Nb. Indeed, subsequent wet chemical analysis of both the as-milled ( $t = 40$  h) and annealed powder confirm the presence of 10–12 wt.% Fe in the milled/annealed product. It may be noted that Fe contamination in ball milling in steel media is not entirely avoidable [19]. Although Fe has negligible solubility in Nb at room temperature [20], isothermal annealing at 900°C may lead to partial dissolution of Fe in the f.c.c.-Nb. Thus, it is plausible that Fe contamination in the present study is responsible for an impurity stabilization of the ordered Nb–Fe solid solution formed due to the isothermal annealing at 900°C for 2 h. However, the evolution of an f.c.c. phase cannot be accounted for by solid state dissolution of Fe in Nb as no binary phase in the Fe–Nb system possesses f.c.c. Bravais lattice in the Nb-rich end and/or at room temperature [20]. In this context, it may be mentioned that the possibility of a similar impurity stabilization of f.c.c.-Nb due to Al (instead of Fe) cannot be ruled out in the case of mechanical alloying of Nb<sub>75</sub>Al<sub>25</sub> powder blend aimed at preparing Nb<sub>3</sub>Al. In fact, Peng et al. [8] also observed that the f.c.c. phase in the Nb<sub>75</sub>Al<sub>25</sub> powder blend was quite stable and did not decompose at high temperature. Perhaps, this b.c.c.  $\rightarrow$  f.c.c. allotropic change in Nb and subsequent impurity stabilization of the Nb-solid solution may be responsible for the inability of producing pure Nb<sub>3</sub>Al by mechanical alloying in steel or WC media.

Finally, the role of impurities, the occurrence of which is fairly common in mechanical alloying, in causing the allotropic change or stabilizing the subsequent ordering reaction, deserves a due consideration at this stage. Since impurities to the maximum levels of 0.11 wt.% nitrogen, 2 wt.%

carbon and 12 wt.% iron have been detected, it is logical to anticipate that either nitride/carbide type of impurity reaction products or Nb–Fe–N–C type of complex compounds may form in the present ball milling routine of elemental Nb. Indeed, the impurities present may influence the solid state phase change. However, the host of counter evidences like (a) the final milled product being single phase, (b) the impurity levels being lower than the minimum amount needed if the end product is a single phase nitride or carbide, (c) the resistivity of the f.c.c. phase being lower than that of the starting material (b.c.c.-Nb) or possible nitrides/carbides of Nb, and (d) the observed lattice parameter (=0.428 nm) being quite small for a Nb–Fe–N–C type of complex compound, appears to suggest that the f.c.c. phase is indeed an allotropic form of Nb (containing a fair amount of dissolved impurities) and not either a simple or complex ceramic phase like nitride, carbide or carbonitride. In the event of a future evidence that the said b.c.c.  $\rightarrow$  f.c.c. change is absent in nanocrystalline Nb (with less than 7–8 nm grain size), it would be pertinent to conclude that the observed f.c.c. phase in the present investigation is a complex compound and not an allotropic state of Nb. This remains an interesting topic of future investigation.

#### 4. Conclusions

Elemental Nb undergoes an irreversible b.c.c.  $\rightarrow$  f.c.c. allotropic transformation when the grain size reduces to below 10 nm during high energy ball milling. This allotropic transformation is preceded by a continuous lattice expansion throughout the ball milling operation. While a fair amount of contamination (Fe, N, C) is detected in the milled product by chemical analysis, it is expected that such impurities may remain mostly dissolved in the end product believed to be f.c.c.-Nb and not a new complex multi-component ceramic compound of Nb. Subsequently, the said f.c.c. phase undergoes possibly an impurity stabilized ordering transformation on annealing at 900°C for 2 h.

#### Acknowledgements

Equipment support from DST, New Delhi (Grant No. III.4 (23) 92-ET) is thankfully acknowledged. PPC is grateful to the QIP scheme of financial support of AICTE, New Delhi.

#### References

- [1] D.M. Dimiduk, M.G. Mendiretta, P.R. Subramanian, in: R. Darolia (Ed.), Structural Intermetallics, TMS, Warrendale, PA, 1993, p. 619.
- [2] S.K. Pabi, B.S. Murty, Mater. Sci. Eng. A 214 (1996) 146.
- [3] S.K. Pabi, J. Joarder, I. Manna, B.S. Murty, Nanostruct. Mater. 9 (1997) 142.
- [4] B.S. Murty, S.K. Pabi, Nanostruct. Mater. 7 (1996) 691.
- [5] M.A. Morris, D.G. Morris, Mater. Sci. Eng. A 136 (1991) 59.

- [6] G.H. Fair, J.V. Wood, *Powder Metall.* 36 (1993) 123.
- [7] E. Hellstern, L. Schultz, R. Bormann, D. Lee, *Appl. Phys. Lett.* 53 (1988) 1399.
- [8] Z. Peng, C. Suryanarayana, F.H. Froes, *Metall. Mater. Trans. A* 27 (1996) 41.
- [9] C. Rock, K. Okazaki, *Nanostruct. Mater.* 5 (1995) 643.
- [10] P.P. Chatterjee, S.K. Pabi, I. Manna, *J. Appl. Phys.* 86 (1999) 5912.
- [11] G. Cocco, I. Soletta, L. Battezzati, M. Baricco, S. Enzo, *Phil. Mag. B* 61 (1990) 446.
- [12] J.Y. Huang, Y.K. Wu, H.Q. Ye, *Acta Metall. Mater.* 44 (1996) 1201.
- [13] B.D. Cullity, *Elements of X-ray Diffraction*, Addison-Wesley, Reading, MA, 1975, p. 102.
- [14] I.L. Langford, *J. Appl. Cryst.* 11 (1978) 10.
- [15] A.A. Ramadan, R.D. Gould, A. Ashahur, *Thin Solid Films* 239 (1994) 272.
- [16] M.L. Jackson, *Soil Chemical Analysis*, Prentice-Hall, New Delhi, 1973, p. 1.
- [17] T.B. Massalski (Ed.), *Binary Alloy Phase Diagram*, 2nd Edition, ASM International, Materials Park, OH, 1990, p. 2692.
- [18] J.F. Smith, O.N. Carlsson, R.R. de Avillez, in: T.B. Massalski (Ed.), *Binary Alloy Phase Diagram*, 2nd Edition, Vol. 1, ASM International, Materials Park, OH, 1990, p. 863.
- [19] C.C. Koch, in: R.W. Cahn, P. Haasen, E.J. Kramer (Eds.), *Materials Science and Technology*, Vol. 15, VCH, Weinheim, 1991, p. 193.
- [20] E. Paul, L.J. Swartzendruber, in: T.B. Massalski (Ed.), *Binary Alloy Phase Diagrams*, 2nd Edition, ASM International, Materials Park, OH, 1990, p. 1733.